Journal of Microscopy

*Journal of Microscopy, Vol. 00, Issue 0 2016, pp. 1–10*
*Received 25 November 2015; accepted 30 May 2016*

doi: 10.1111/jmi.12439

# Miniaturized modules for light sheet microscopy with low chromatic aberration

T. BRUNS*, M. BAUER†, S. BRUNS*, H. MEYER†, D. KUBIN‡ & H. SCHNECKENBURGER*

*Aalen University, Institute of Applied Research, Beethovenstr. 1, 73430, Aalen, Germany

†J&M Analytik AG, Willy-Messerschmitt-Straße 8, 73457, Essingen, Germany

‡JM Microsystems GmbH, Willy-Messerschmitt-Straße 8, 73457, Essingen, Germany

**Key words.** Achromatic illumination modules, astigmatism, light sheet fluorescence microscopy, multicellular tumour spheroids, single plane illumination microscopy.

## Summary

Two miniaturized fibre-coupled modules for light sheet-based microscopy are described and compared with respect to image quality, chromatic aberration and beam alignment. Whereas in one module the light sheet is created by an achromatic cylindrical lens, reflection by a spherical mirror and concomitant astigmatic distortion are used to create the light sheet in the second module. Test experiments with fluorescent dyes in solution and multicellular tumour spheroids are reported, and some details on construction are given for both systems. Both modules are optimized for imaging individual cell layers of 3D biological samples and can be adapted to fit commercial microscopes.

## Introduction

In recent years, light sheet microscopy has proven to be a valuable method for 3D imaging of biological specimens (Huisken *et al.*, 2004; Santi, 2011). In contrast to established methods, e.g. confocal laser scanning microscopy (Pawley, 1990; Webb, 1996) or structured illumination microscopy (Neil *et al.*, 1997; Gustafsson *et al.*, 2008), samples are illuminated perpendicular to the detection path by a light sheet which is commonly created by a cylindrical lens or by scanning of a laser beam. If either the light sheet or the sample is moved in axial direction, individual planes can be recorded successively with each plane being exposed only once to laser irradiation. This minimizes light exposure of the whole sample and reduces photobleaching and phototoxic damage to living cells or tissues (Schneckenburger *et al.*, 2012; Pampaloni *et al.*, 2015), in particular for long observation times.

Generally, illumination by individual laser wavelengths is described in the literature. Simultaneous illumination by various wavelengths, however, may create longitudinal chromatic aberration resulting e.g. in a focal shift of -780 $\mu$m between wavelengths of 480 and 640 nm, if a singlet planoconvex cylindrical lens made of N-BK 7 with an Abbe number $\nu_e = 64$ and a focal length f' = 50 mm is used. Such a focal shift is crucial in light sheet microscopy since there is a major impact on illumination and thus on image quality. Therefore, some correction is needed for multiwavelength excitation. An easy way of correction is to use individual telescopes for each excitation source, as reported by Schickinger *et al.* (2013) for nanosecond ratio imaging. This, however, makes the experimental setup rather complex. A Galilei telescope, as reported by Bruns *et al.* (2012) appears to be more appropriate for this purpose, but the lack of lenses with appropriate Abbe numbers may prevent its application. Another solution to circumvent chromatic aberration in light sheet microscopy presented by Greger *et al.* (2007) is to use a singlet cylindrical lens that focuses the light into the back focal plane of a well-corrected microscope objective lens. However, in view of miniaturizing the whole system, this technique appears less compact and cost-intensive. Therefore, a commercial achromatic cylindrical lens in combination with an achromatic lens for collimation of light from a glass fibre is presently used to generate the light sheet in a miniaturized illumination module. Alternatively, the exit plane of the illuminating fibre is imaged by a spherical concave mirror with concomitant astigmatic distortion. If light is focused in the sagittal sectional plane of this mirror, a light sheet is formed in its meridional plane without chromatic aberration.

In this paper, the two miniaturized fibre-coupled modules for light sheet microscopy — based on focusing by an achromatic cylindrical lens (lens system) or by a concave spherical mirror (mirror system) — are compared with respect to image quality, chromatic aberration and beam alignment. Test experiments with fluorescent dyes in solution and multicellular tumour spheroids expressing a membrane-associated green fluorescent protein (GFP) are reported, and some details on

Correspondence to: Herbert Schneckenburger, Aalen University, Institute of Applied Research, Beethovenstr. 1, 73430 Aalen, Germany. Tel: +49-7361-576-3401; fax: +49-7361-576-3318; e-mail: herbert.schneckenburger@hs-aalen.de

construction are given. Both setups are characterized by comparably low numerical apertures of illumination resulting in a theoretical waist of the light sheet around 6 $\mu$m and a depth of focus of 40−100 $\mu$m. These setups are optimized for imaging individual cell layers of 3D biological samples and can be adapted to fit commercial microscopes.

## Materials and methods

### *Materials*

For test experiments we used

- Rhodamine 6G prepared as a stock solution of 250 $\mu$M in ethanol and further diluted in bidistilled water to a concentration of 25 $\mu$M. This solution was filled into rectangular glass capillaries of 600 $\mu$m inner diameter and a wall thickness of 120 $\mu$m which were used for light sheet fluorescence microscopy, as described elsewhere (Bruns *et al.*, 2012);
- Multicellular tumour spheroids of Chinese hamster ovary cells permanently transfected with a plasmid encoding for a membrane-associated GFP (CHO-pAcGFP1-Mem). Cells were grown in low-melting agarose (0.5% in culture medium RPMI 1640 without supplements) covered with culture medium RPMI 1640 (supplemented with 10% FBS, 1% penicillin/streptomycin and 500 $\mu$g/mL G 418-BC) up to a size of about 100 $\mu$m. For light sheet fluorescence microscopy, microcapillaries (same as above) were loaded with individual spheroids by plunging the capillaries into the agarose.

### *Light sheet microscopy*

For illumination a photonic crystal fibre laser (NKT Photonics SuperK EXTREME with SuperK VARIA tunable single line filter) operated at 470 nm (bandwidth 10 nm) is used in combination with a single mode fibre (Thorlabs, P1-460B-FC-5) of about 3.3 $\mu$m mode field diameter. Light sheet modules (lens system or mirror system) are mounted to an inverted microscope (Zeiss Axiovert 200M), and fluorescence images are recorded by a CCD camera (Zeiss AxioCam MRc) using a long pass filter for $\lambda \geq 515$ nm and a 10×/0.3 objective lens (Zeiss EC Plan-Neofluar).

In the lens system, the divergent beam of the fibre is deflected by a mirror and collimated by an achromatic lens with a focal length of 25 mm (Qioptiq, G052007000), thus resulting in a parallel beam of about 6 mm in diameter passing an aperture A = 4 mm, as depicted in Figure 1 (A, B). With a focusing achromatic cylindrical lens – consisting of a biconvex and a concave-convex lens – of 25 mm focal length (Edmund Optics, #68-160, N-BK7/N-SF5) a numerical aperture $A_N = 0.08$ is attained when using the relation $A_N = \sin\alpha \approx \tan\alpha = A/2f'$ for small angles. The resulting beam waist $d = \lambda/A_N = 5.9$ $\mu$m is defined by the thinnest line described by the distance between the first zeros of the diffraction function of a slit. The depth of focus $L = n\lambda/A_N^2$ considered in physical optics as the length in direction of light propagation within which the beam waist broadens by 20% is about 100 $\mu$m (with $\lambda = 470$ nm and $n = 1.33$). In test experiments with fluorescent dyes and multicellular spheroids, broadening of the beam waist to less than 10 $\mu$m (corresponding to the thickness of a single cell layer) is used as a criterion for confinement of the light sheet. The chromatic focal shift calculated for the lens pair by Zemax simulation is -60 $\mu$m between wavelengths of 470 and 600 nm and -140 $\mu$m between 440 and 550 nm. These values have been confirmed experimentally.

The light sheet and detection lens can be shifted simultaneously in axial direction using a mechanical coupler between the illumination unit (1) in Figure 1 and the z-stage of the objective turret as described by Bruns *et al.* (2014). This coupler permits to move the illumination unit (and therefore the light sheet) and the detection lens by a different feed factor to compensate for the so-called fish tank effect. This effect describes

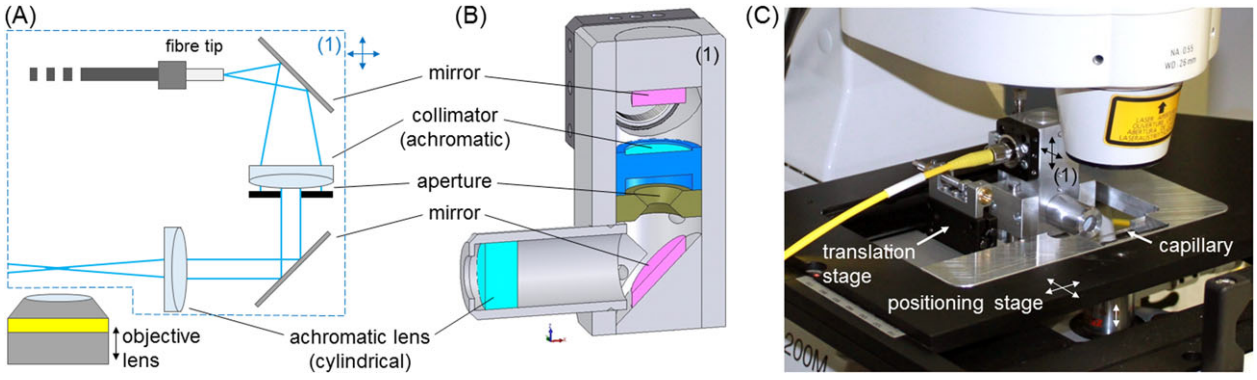


**Fig. 1.** Light sheet illumination using fibre optics in combination with an achromatic cylindrical lens; (A) schematic; (B) technical setup of the illumination unit; (C) adaptation to an inverted microscope. The arrows indicate in which directions the illumination unit (1), the detection lens and the capillary can be moved.

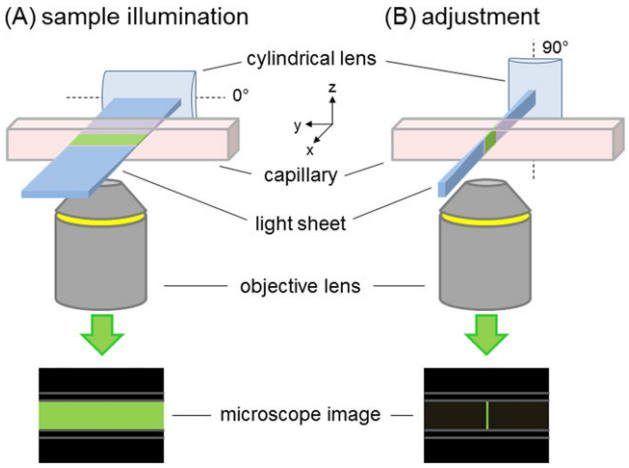


**Fig. 2.** Sample illumination (A) and adjustment (B) of the light sheet (upon rotation of the cylindrical lens by 90°). For both cases, the microscope images are depicted schematically. Whereas the left image shows the light sheet, the right image shows the beam waist in direction of light propagation.

the difference of optical pathways in media with different refractive indices, e.g. the cell (with the surrounding medium) and air. The ratio between the shifts of the focal plane and the detection lens $\Delta z_{foc}/\Delta z_{lens}$ is, therefore, given by the ratio of aperture angles $\tan \sigma_{air}/\tan \sigma_{cell}$, and for small apertures of the detection lens can be approximated by the refractive index ratio $n_{cell}/n_{air}$.

The whole setup for light sheet illumination with a size around $8 \times 7 \times 6$ cm$^3$ can be mounted to the fixed part of the positioning stage of a commercial microscope with a mechanical adapter, but without any further modification of the microscope. The capillary containing the sample is placed in a sample holder inserted in the movable part of the positioning stage, as depicted in Figure 1(C).

Adjustment of the light sheet is depicted in Figure 2. The aim of this adjustment is to check whether the light sheet is focused above the objective lens to ensure optimum illumination of the sample. For this purpose, a capillary filled with a fluorescent dye, e.g. rhodamine 6G, is placed in the sample holder. The cylindrical lens is now rotated by 90° to visualize the beam waist and to adjust its position by moving the illumination unit via a translation stage back and forth in horizontal direction. Finally, the cylindrical lens is rotated back to its initial position for illumination of the samples.

In the mirror system depicted in Figure 3, the exit plane of the illuminating fibre is imaged into the specimen with a magnification m = -1 by a spherical concave mirror with a radius of curvature of 50.8 mm resulting in a focal length of 25.4 mm. Since the object is positioned outside the optical axis of the mirror, astigmatic distortion occurs with a meridional ($I_M$) and a sagittal ($I_S$) image plane. In the sagittal image plane, the meridional beam is defocused, resulting in a light sheet of about 4 mm width depicted schematically in Figure 3(A). Whereas the mechanical setup for light sheet generation is depicted in Figure 3(B), the whole module mounted to the positioning stage of an inverted microscope is shown in Figure 3(C). The numerical aperture of the excitation beam in the sample corresponds to the numerical aperture $A_N = 0.12$ of the fibre and causes a diffraction limited light sheet of $d = 4.8$ $\mu$m thickness in the sagittal image plane according to $d = 1.22\lambda/A_N$ with $\lambda = 470$ nm. Geometrical imaging of the exit face of the fibre core (mode field diameter: 3.3 $\mu$m, defined by the manufacturer as beam diameter at the $1/e^2$ level of the Gaussian profile) with a magnification $m = -1$ and diffraction results in an effective beam waist of about 7 $\mu$m (full line width). In contrast to the lens system, the illumination unit and the capillary holder are both motorized in the mirror system and can be controlled independently to compensate for the fish tank effect. This means that for recording individual planes of the sample, the sample is moved through the focal plane of the objective lens whereas the light sheet is readjusted in $z$-direction (perpendicular to the direction of illumination).

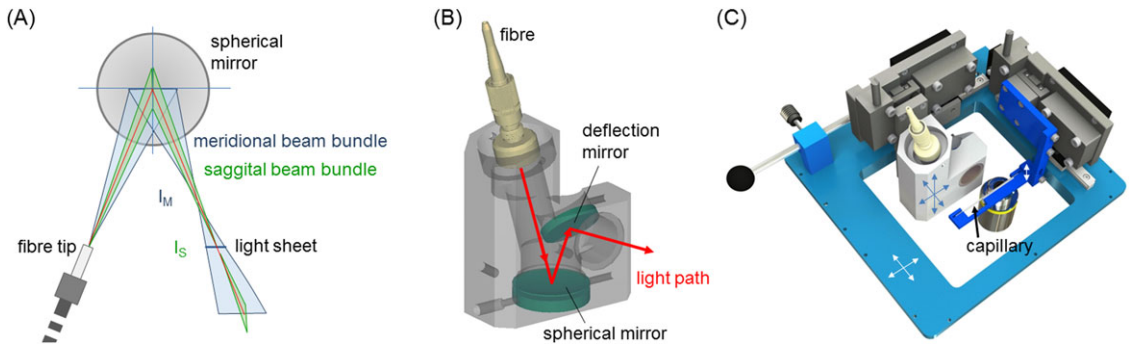


**Fig. 3.** Light sheet illumination using reflection by a spherical mirror and concomitant astigmatic distortion; (A) schematic with image planes $I_M$ (meridional) and $I_S$ (sagittal); (B) mechanical setup of the illumination unit; (C) motorized light sheet module to be mounted to the positioning stage of an inverted microscope. The arrows indicate the directions in which the single components of the module as well as the whole module can be moved. Only the movement in axial direction (direction of detection) is motorized.

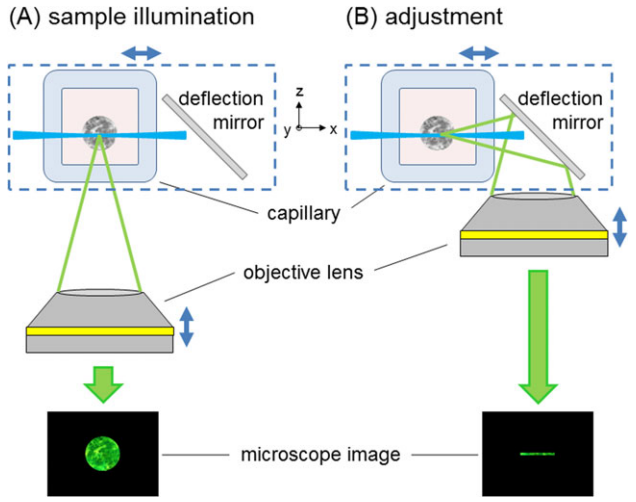


**Fig. 4.** Sample illumination (A) and light sheet adjustment (B) upon observation of the sample from the side via a deflection mirror (moving the positioning stage in lateral and the objective lens in axial direction as indicated by the arrows). Whereas the left image shows the whole optical slice of the sample, the right image shows the width of the light sheet across the sample.

Using an additional mirror next to the capillary, the light sheet can be adjusted for minimum beam waist in the plane of the sample. The positioning stage of the microscope – where the whole module is mounted – is moved towards the direction of light propagation until the deflection mirror attached to the capillary holder reflects the excitation light towards the objective lens of the microscope as depicted in Figure 4(B). This setup enables the user to view the fluorescence originating from the illuminated part of the sample (possibly superposed by some minor amount of excitation light) from the side.

## Results

Exemplary results obtained with the lens system are depicted in Figure 5. In Figure 5(A), the profile of the light sheet in the direction of beam propagation ($x$-direction) is visualized in a rhodamine 6G solution using the adjustment configuration of Figure 2(B). Recording of an intensity profile across the beam results in a beam waist of 6 $\mu$m (full width at half maximum; FWHM) in the focus of the cylindrical lens, which is in agreement with theoretical calculations. The FWHM is broadened to 9−10 $\mu$m at a distance of −100 $\mu$m in front or +100 $\mu$m behind this focus. This proves that the thickness of the light sheet can be kept below 10 $\mu$m over a sample diameter of about 200 $\mu$m. A multicellular spheroid of CHO-pAcGFP1-Mem cells upon transillumination is depicted in Figure 5(B), whereas individual planes illuminated by a light sheet are demonstrated in Figures 5(C−E). These images document very well the green fluorescent cell membranes within each layer.

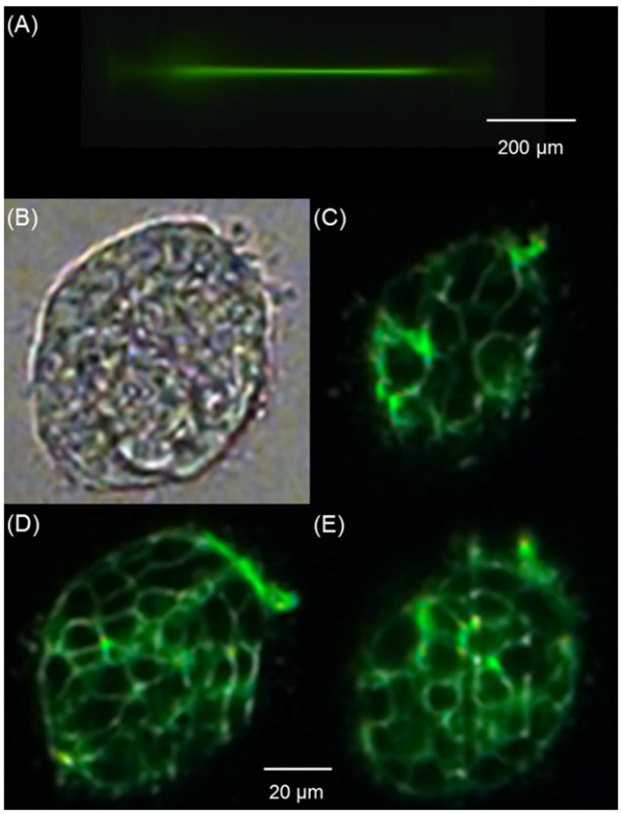


**Fig. 5.** Light sheet illumination by the lens system; (A) longitudinal beam profile ($x$-direction) in a rhodamine 6G solution; (B) multicellular spheroid of CHO-pAcGFP1-Mem cells upon transillumination; (C−E) individual cell layers upon light sheet illumination with intervals $\Delta z = 21$ $\mu$m and thickness $d \leq 10$ $\mu$m. Scale bars are indicated separately for Figure 5(A) and Figures 5(B−E).

Results obtained with the mirror system are depicted in Figure 6. In Figure 6(A), the light sheet is again visualized in a rhodamine 6G solution, but in perpendicular direction to beam propagation (transverse beam profile, $y$-direction), corresponding to the adjustment configuration of Figure 4(B). A green seam on both sides of the light sheet results from scattering and causes spreading of the FWHM to about 11 $\mu$m. Figure 6(B) shows again a multicellular spheroid of CHO-pAcGFP1-Mem cells upon transillumination, whereas in Figure 6(C−E), individual planes illuminated by a light sheet are depicted. These images document once more the green fluorescent cell membranes within each layer.

In contrast to Figure 6(A) an FWHM of about 7 $\mu$m – corresponding to the theoretical value – was obtained for the mirror system upon dismantling the illumination unit from the motorized stage and rotating it by 90° so that the profile in direction of beam propagation ($x$-direction, longitudinal profile) could be visualized, as depicted in Figure 7. This experiment also proved that a thickness of the light sheet (FWHM) below 10 $\mu$m is maintained over a distance of about

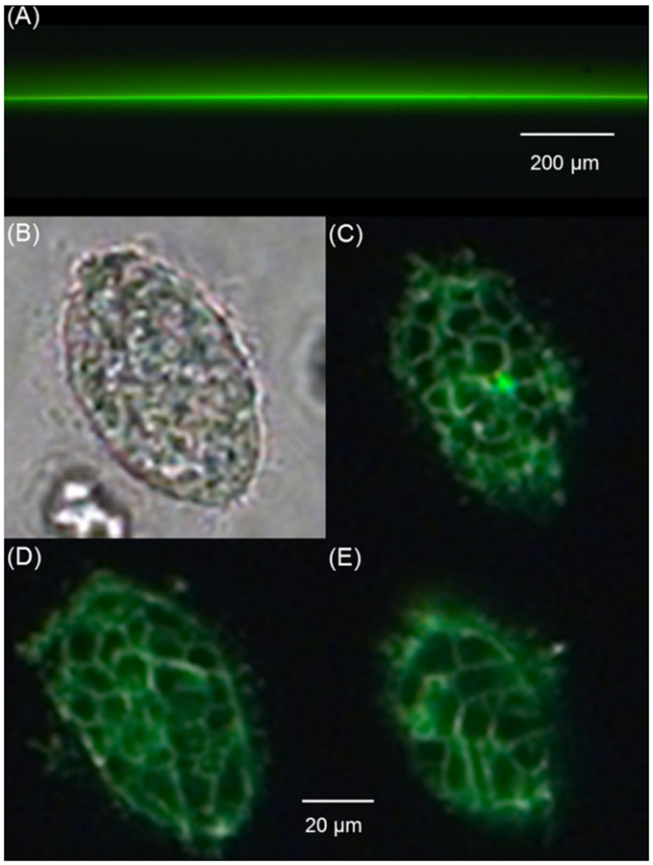


**Fig. 6.** Light sheet illumination by the mirror system; (A) transverse beam profile ($y$-direction) in a rhodamine 6G solution; (B) multicellular spheroid of CHO-pAcGFP1-Mem cells upon transillumination; (C–E) individual cell layers upon light sheet illumination with intervals $\Delta z = 21\ \mu$m and thickness $d \leq 10\ \mu$m. Scale bars are indicated separately for Figure 6(A) and Figures 6(B–E).

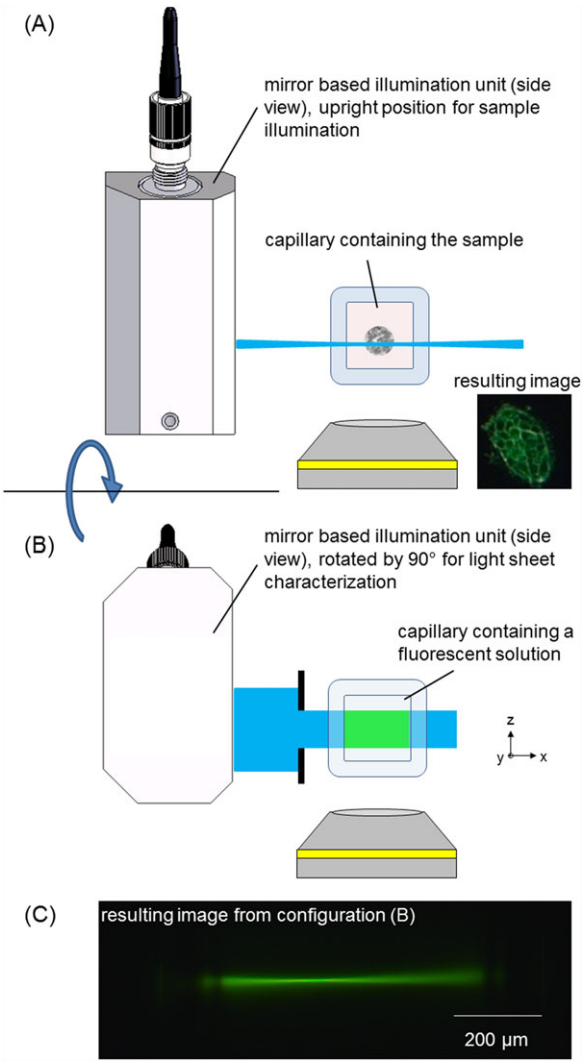


**Fig. 7.** Mirror-based illumination unit in upright position for sample illumination (A) and rotated by 90° (as indicated by the arrow) for measurement of the longitudinal beam profile ($x$-direction, B). Rotation of the illumination unit is only possible when dismantled from the motorized stage. (C) Resulting longitudinal beam profile in $x$-direction in a rhodamine 6G solution.

140 $\mu$m, i.e. from −70 $\mu$m in front up to +70 $\mu$m behind the focus.

## Discussion

Two miniaturized modules for light sheet illumination – based on imaging by an achromatic lens or by a spherical mirror and concomitant astigmatic distortion – are described. Both modules can be integrated into the positioning stage of a commercial inverted microscope and permit versatile light sheet imaging including 3D, spectral and fluorescence lifetime imaging. Using microcapillaries for localization of cell or tissue samples or even small organisms, experiments can be performed under stationary or microfluidic conditions with very low amounts of culture media or reagents, e.g. fluorescent dyes or cytostatic drugs (Bruns *et al.*, 2014). Also, sample rotation as reported by Bruns *et al.* (2015) is easy to perform, if observation from different sides is desirable.

Regarding axial resolution, both setups have been optimized for imaging single cell layers up to 10 $\mu$m thickness in 3D cell systems. This thickness can be maintained over a longitudinal distance up to 200 $\mu$m for the lens system and about 140 $\mu$m for the mirror system using a numerical aperture $A_N = 0.08$ in the first case and $A_N = 0.12$ in the second case. Thinner light sheets – and therefore higher axial resolution – can be achieved by the lens system, if the aspheric cylindrical lens focuses the light into the back focal plane of a microscope objective lens with higher numerical aperture, as reported by Greger *et al.* (2007). However, whether this extension of the illumination unit is reasonable mainly depends on the application as well as on the size and the state of the specimen to be examined since

higher numerical apertures of illumination result in shorter depths of focus $L = n\lambda/A_N^2$. For homogeneous illumination, it may be desirable that the depth of focus of the illumination beam vaguely matches the diameter of the sample.

For detection, a larger number of objective lenses with working distances above 1 mm can be used. Lateral resolution is the same as for conventional wide-field microscopy, whereas the image contrast is enhanced upon selective illumination of individual layers. Light sheets of similar quality are generated for both miniaturized illumination modules. Chromatic aberration is eliminated in the mirror system, if aberrations within the glass walls or the culture media are negligible, i.e. if these layers are thin enough. On the other hand, longitudinal chromatic aberration has been minimized, but is still present in the lens system, causing a focal shift of about 140 $\mu$m when the excitation wavelength is varied in the range of 440–550 nm. Therefore, some minor readjustment is needed when changing the excitation wavelength. This favours the mirror system in view of light sheet microscopy free of chromatic aberration. However, easier handling and adjustment as well as the possibility to exchange the focusing (cylindrical) lens are major advantages of the lens system. Possibly, a hybrid system based on the setup depicted in Figure 1 with a focusing mirror instead of the collimating lens would combine reduced chromatic aberration with easy handling and adjustment.

In principle there are no restrictions considering the light source or the light transmission system. Although both modules are optimized for typical apertures of single mode fibres, other types of fibres or even free laser beams are applicable. Applications without considering laser safety may be opened up by use of a light emitting diode in combination with a narrow slit that is imaged into the specimen instead of laser illumination. This technique was tested with the mirror system by replacing the fibre tip by a light emitting diode (Thorlabs, LED470L, $\lambda = 470 \pm 11$ nm, optical power 170 mW) mounted in front of a 10 $\mu$m slit using the same imaging system as depicted in Figure 3. The illumination unit of the mirror system is designed in such a way that the two kinds of light sources can be exchanged easily. In comparison with laser excitation, the width of the beam is broadened from 4 to about 9 mm due to geometrical imaging of the slit. Results are documented in Figure 8 showing the transverse beam profile ($y$-direction) of the light emitting diode-induced light sheet of 11 $\mu$m (FWHM) generated by the mirror system (experimental setup as shown in Figure 4(B) as well as fluorescence images of single spheroid layers.

In summary, both light sheet modules reported above appear to be versatile and low-cost alternatives to commercial light sheet microscopes. The modules can be mounted to a variety of inverted microscopes from different manufacturers (e.g. Zeiss Axiovert 200M, Leica DMi8). They provide high flexibility and multiple detection modes including 3D imaging, spectral imaging and fluorescence lifetime imaging. Moreover, further features of the microscope, e.g. laser scanning or wide-field modes can still be used without any modifications. The eyepiece can be used for rapid sample localization and adjustment of the light sheet in relation to the sample. Presently, a nonmotorized setup is reported for the lens system, using a mechanical coupler between the $z$-stage of the objective turret and the illumination unit to enable simultaneous shifts of the light sheet and the detection lens, while a motorized shift of the sample in combination with motorized readjustment of the light sheet is reported for the mirror system. However, in general, both illumination units can be used with the motorized or the nonmotorized setup.

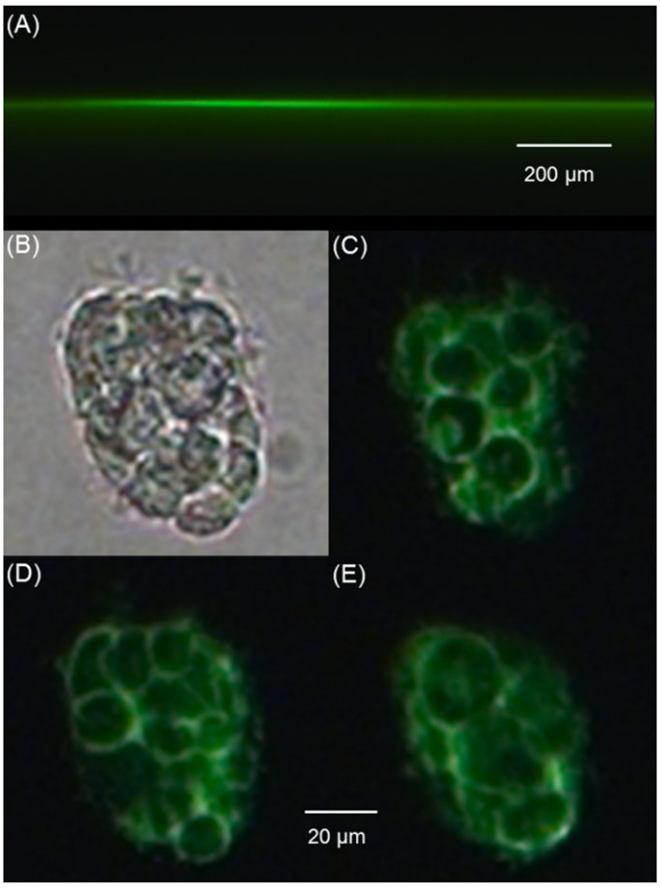


**Fig. 8.** Light sheet illumination by the mirror system in combination with a light emitting diode; (A) transverse beam profile ($y$-direction) in a rhodamine 6G solution; (B) multicellular spheroid of CHO-pAcGFP1-Mem cells upon transillumination; (C–E) individual cell layers upon light sheet illumination with intervals $\Delta z = 14$ $\mu$m. Scale bars are indicated separately for Figure 7(A) and Figures 7(B–E).

**Acknowledgement**

This project was funded by the Land Baden-Württemberg, the European Union, Europäischer Fonds für die Regionale Entwicklung as well as the Bundesministerium für Wirtschaft und

Energie (BMWi), Zentrales Innovationsprogramm Mittelstand ZIM (grant no. KF 2888104UW3). The authors thank Michael Wagner for performing Zemax simulations of the achromatic lens system and Claudia Hintze for skilful technical assistance.

## References

Bruns, T., Schickinger, S., Wittig, R. & Schneckenburger, H. (2012) Preparation strategy and illumination of 3D cell cultures in light sheet-based fluorescence microscopy. *J. Biomed. Opt.* **17**, 101518-1–10518-5.

Bruns, T., Schickinger, S. & Schneckenburger, H. (2014) Single plane illumination module and micro-capillary approach for a wide-field microscope. *J. Vis. Exp.* **15**(90), e51993-1–e51993-10.

Bruns, T., Schickinger, S. & Schneckenburger, H. (2015) Sample holder for axial rotation of specimens in 3D microscopy. *J. Microsc.* **260**(1), 30–36.

Greger, K., Swoger, J. & Stelzer, E.H.K. (2007) Basic building units and properties of a fluorescence single plane illumination microscope. *Rev. Sci. Instrum.* **78**, 023705-1–023705-7.

Gustafsson, M.G.L., Shao, L., Carlton, P.M., Wang, C.J., Glubovskaya, I.N., Cande, W.Z., Agard, D.a. & Sadat, J.W. (2008) Three-dimensional resolution doubling in wide-field fluorescence microscopy by structured illumination. *Biophys. J.* **94**(12), 4957–4970.

Huisken, J., Swoger, J., del Bene, F., Wittbrodt, J. & Stelzer, E.H.K. (2004) Optical sectioning deep inside live embryos by SPIM. *Science* **305**(5686), 1007–1009.

Neil, M.A., Juskaitis, R. & Wilson, T. (1997) Method of obtaining optical sectioning by using structured light in a conventional microscope. *Opt. Lett.* **22**(24), 1905–1907.

Pampaloni, F., Chang, B.-J. & Stelzer, E.H.K. (2015) Light sheet-based fluorescence microscopy (LSFM) for the quantitative imaging of cells and tissues. *Cell Tissue Res.* **362**(1), 265–277.

Pawley, J. (1990) *Handbook of Biological Confocal Microscopy*. Plenum Press, New York.

Santi, P.A. (2011) Light sheet fluorescence microscopy: a review. *J. Histochem. Cytochem.* **59**(2), 129–138.

Schickinger, S., Bruns, T., Wittig, R., Weber, P., Wagner, M. & Schneckenburger, H. (2013) Nanosecond ratio imaging of redox states in tumor cell spheroids using light sheet-based fluorescence microscopy. *J. Biomed. Opt.* **18**(12), 126007-1–126007-5.

Schneckenburger, H., Weber, P., Wagner, M., Schickinger, S., Richter, V., Bruns, T., Strauss, W.S.L. & Wittig, R. (2012) Light exposure and cell viability in fluorescence microscopy. *J. Microsc.* **245**, 311–318.

Webb, R.H. (1996) Confocal optical microscopy. *Rep. Prog. Phys.* **59**, 427–471.